Jurnal Pertahanan

SN-CUO-ARABIC GUM COMPOSITION FOR RED TRACER PROJECTILE AMMUNITION POTENTIAL

Abdul Basyir[1], Nining Sumawati Asri[2], Didik Aryanto[3], Isnaeni[4], Cherly Firdharini[5], Wahyu Bambang Widayatno[6], Agus Sukarto Wismogroho[7]
Research Center for Physics, Indonesian Institute of Sciences
440 – 442 Building, Puspiptek Area, Muncul, Setu, South Tangerang, Banten, Indonesia 15314
abdu077@lipi.go.id[1], nini008@lipi.go.id[2], didi027@lipi.go.id[3], isna001@lipi.go.id[4],
cfirdharini96@gmail.com[5], wahy012@lipi.go.id[6], agus046@lipi.go.id[9]

Diang Sagita[8]
Research for Appropriate Technology, Indonesian Institute of Sciences
Cigadung Area, Subang City, West Java, Indonesia 41213
dian043@lipi.go.id[8]

Denny Lesmana[9]
Ammunition Division, Pindad Ltd. (Persero)
General Sudirman Street, Turen, Malang, East Java, Indonesia 65175
dennyl@pindad.com[9]

Article Info

Abstract

Fundamentally, tracer projectile material based on pyrotechnic composition, and where the pyrotechnic was generally composed of fuel, oxidizer, and binder. The tin (Sn) material is one of the candidates for fuel material because tin has a low melting point, so this composition can ignite at low temperature, while the copper oxide (CuO) can emit the orange-red spectrum. This study aims to evaluate the thermal and spectrum character of Sn-CuO-AG-based composition. The characterization data of these samples was evaluated by tests of morphology and phase, enthalpy change, calorie energy, and spectrum emission. Based on this data, the 17Sn-68CuO-15AG sample was emitted a strong red color too, but this sample has a high or the longest exothermic process. Furthermore, the 27Sn-58CuO-15AG sample has emitted a weak red color with medium exothermic energy. Generally, the 22Sn-63CuO-15AG is more suitable than the two other compositions for the tracer projectile composition of ammunition, this material emits a strong red spectrum and low-calorie energy.

INTRODUCTION

Material science has an important role in defense technology development. Some aspects were involving material science such as material for the propulsion systems, warheads, and frames in rockets and missiles, armor in personal and vehicles, frame or body in vehicles, energetic materials in ammunition, etc. (Agrawal, 2010; Crouch, 2019; National Research Council, 2003). Especially for ammunition, material research was related to reliable material for components of ammunition such as projectile, casing, and propellant.

One type of component on the projectile is the tracer projectile. Generally, this component is added to the back of the core projectile. So, when the projectile going to the target, at the back of this projectile can be seen a luminous color. Therefore, this component can be used as a trajectory signal from the projectile, a strategy in the war, the marker of ammunition stock in the weapon, and the marker of enemy position (Garner, Huang, Mishock, & Kostka, 2009). Furthermore, this tracer projectile can be also used as an explosive trigger on vehicle enemy, because this component can generate heat energy and sparks to ignite a fire.

Pyrotechnic is a basic concept in creating material formulation of tracer projectile, and where this component was composed of fuel, oxidizer, color source, and binder material (Agrawal, 2010). Generally, fuel material consisted of metal and non-metal such as magnesium, aluminum, boron, silicon, and others. Furthermore, magnesium and aluminum are the materials that are often used as fuel. Meanwhile, oxidizer and color source material is arranged of nitrate, iodate, chlorate/ perchlorate, chromate/ dichromate, oxide/ peroxide, and halocarbon group. The strontium-based, natrium-based, and barium-based materials were usually used as red, yellow, and green color for tracer projectile (Sadek, Kassem, Abdo, & Elbasuney, 2016, 2017).

Moreover, binder material was divided into natural and synthetic binders (Bailey & Murray, 2000; Conkling & Mocella, 2019; Ellern, 1968).

Based on the sensitivity of the eye, the retina contained two types of photo-sensitive elements, photopic-eye and scotopic-eye response (Buc, Adelman, & Adelman, 1993), and where the photopic-eye and scotopic-eye response is more sensitive at daylight and night, respectively. Furthermore, the scotopic-eye response is more sensitive than the photopic-eye response, but the ability to separate color is not good. However, the eye can see the red color in the night better than the green, blue, and yellow color. So, in the night condition, the user of the red tracer projectile can see the trajectory of their projectile to the target is clearer than used green, blue, or yellow tracer projectile. Therefore, this research will synthesize, characterize, and analyze material formulation for a red-tracer projectile candidate.

All material generates luminescence, only different in the intensity and wavelength of the spectrum. Furthermore, the different material generates different heat energy, and where the high heat energy and temperature ignite can cause the broken and/or crack at the projectile jacket. This break can be affected by projectile accuracy, and further, this problem can cause injury to the user of this tracer projectile. Therefore, the parameter of quality of color and temperature ignites level – heat energy level is used to determine the quality of the tracer projectile.

In this research, the tin (Sn) material is used as the fuel material, while the copper oxide (CuO) is the oxidizer-color source and Arabic Gum (AG) material as a binder. The Sn material is chosen as fuel material in this research because the Sn has a low melting point, around 232° C. Furthermore, Indonesia is the second-largest tin producer in the world, after China, so that tin resources in Indonesia

very much (Anderson, 2020; ITRI, 2020). The low melting point of fuel material, expected to produce low temperature ignites for this composition.

Meanwhile, the CuO material is chosen as an oxidizer-color source because the CuO material emitted a spectrum in the red region, and this emits was usually seen at the top of the blue flame, spectrum range of 610 – 720 nm (Meyerriecks & Kosanke, 2003), and/or this material emitted a strong orange color and weak green color (Douda, 1964), while the copper material was the color source for blue color (Conkling & Mocella, 2019; Ellern, 1968). Moreover, the AG is chosen as a binder because based on our research previously, between Arabic Gum (AG), Poly Vinyl Chloride (PVC), and dextrin, the binder of AG can generate pellets smoother than PVC and dextrin, without crack on the surface of pellets. Furthermore, the AG material was found to be a novel binder for red tracer and an effective binder to enhance color quality and light intensity (Sadek et al., 2017).

Based on the explanation, this research expected to generate the composition for red tracer projectile candidates with low-calorie energy and strong signals in the red spectrum. This character can help the user to avoid a shooting fail accident because the low-calorie energy can reduce crack in the jacket. Meanwhile, the strong red spectrum of tracer projectile can enhance the sign to the friend regarding the location of the enemy.

METHODS

Synthesize of tracer projectile used a combination between mechanical alloying (MA) method and automatic pressing method. The tracer projectile material was composed of tin (Sn) (generated by Research Center for Physics through hot gas atomization method and with the particle size of < 25 μm), copper (II) oxide (CuO) (Code: CTE54-100, Pudak Scientific), and Arabic gum AG) (Code: TIC Gums), and where these materials as

fuel, oxidizer – color source, and binder, respectively. After that, the composition of this powder was measured by KERN weighing scales and balances (ABS-220-4N type), refer to this composition, Sn (17, 22, and 27 weight %), CuO (68, 63, and 58 weight %), and AG (15 weight %).

The powder composition amount of 25 grams was mixed for 2 hours (2 minutes on and 5 minutes off) using high-energy milling (PPF-Ultimate Gravity), where the oscillation frequency of this machine is 700/minute. The dry milling was carried out in the cylindrical steel vial (125 ml in volume), and balls mill to powder weight ratio of 4:1. The balls mill in this research used zirconia balls. Furthermore, the zirconia has high hardness, so the powder in this milling process can be avoided of the ball and cylindrical tube contamination. After that, the MA powder amount of 1.5 gram was pressed under auto-machine press (Carver Auto Series NE type) with a load of 8 tons, along 90 seconds. Therefore, this process generated three types of tracer projectile candidates in pellets form.

This sample in this research was characterized refer to these measurements below:

1. The morphology sample was measured by a 3D optical microscope (Keyence VHX-6000). The observation at the sample was used full coaxial light setting, and where this setting can separate the different colors, better than full ring light setting. This sample was measured at magnification 300×, 500×, and 1000×. Furthermore, the morphology of the sample was saved in a jpeg file.

2. The phase of the sample was measured by X-Ray Diffraction (XRD) Rigaku Smartlab with A-26 Cu x-ray tube (1.541862 Armstrong). The setting of this measurement used a scan speed of 5 degrees per minute, with a range of 10 – 90 degrees. Further, the voltage and current tube of this machine used a voltage of 40 kV and a current of 30

mA. Meanwhile, the phase analysis used Smartlab software with a database of PDF4. Moreover, the XRD data was plotted at Origin 2018 software.

3. The density of the sample was measured based on the equation of $\rho = m/v$. The mass of pellets was measured by KERN weighing scales and balances (ABS-220-4N type). While the volume of pellets was measured refer to the tube volume equation, and where the diameter (d) of pellets was measured by screw micrometer (Toki type).

4. The thermal phenomenon and calorie energy at the sample were measured by differential thermal analysis (DTA) (Research Center for Physics – Indonesian Institute of Science type) and Parr 1341 Oxygen Bomb Calorimeter, respectively. For the DTA

test, this measurement used a temperature maximum of 1000° C and a heating rate of 10° C per minute. The volume of the sample for this measurement is around 0.25 cm^3, and this measurement used an alumina tube as a reference.

5. The spectrum of the sample was measured by a spectrometer (Maya2000 Pro series). This measurement was performed at a dark tunnel with a length of 1 meter, and where the sample was burned by Liquified Butane Fuel tube (Super Cook type). After 1 – 2 minutes, this spectrum of each sample can record.

Simply, the process of synthesis and characterization in this research can be seen in the flowchart in Figure 1.
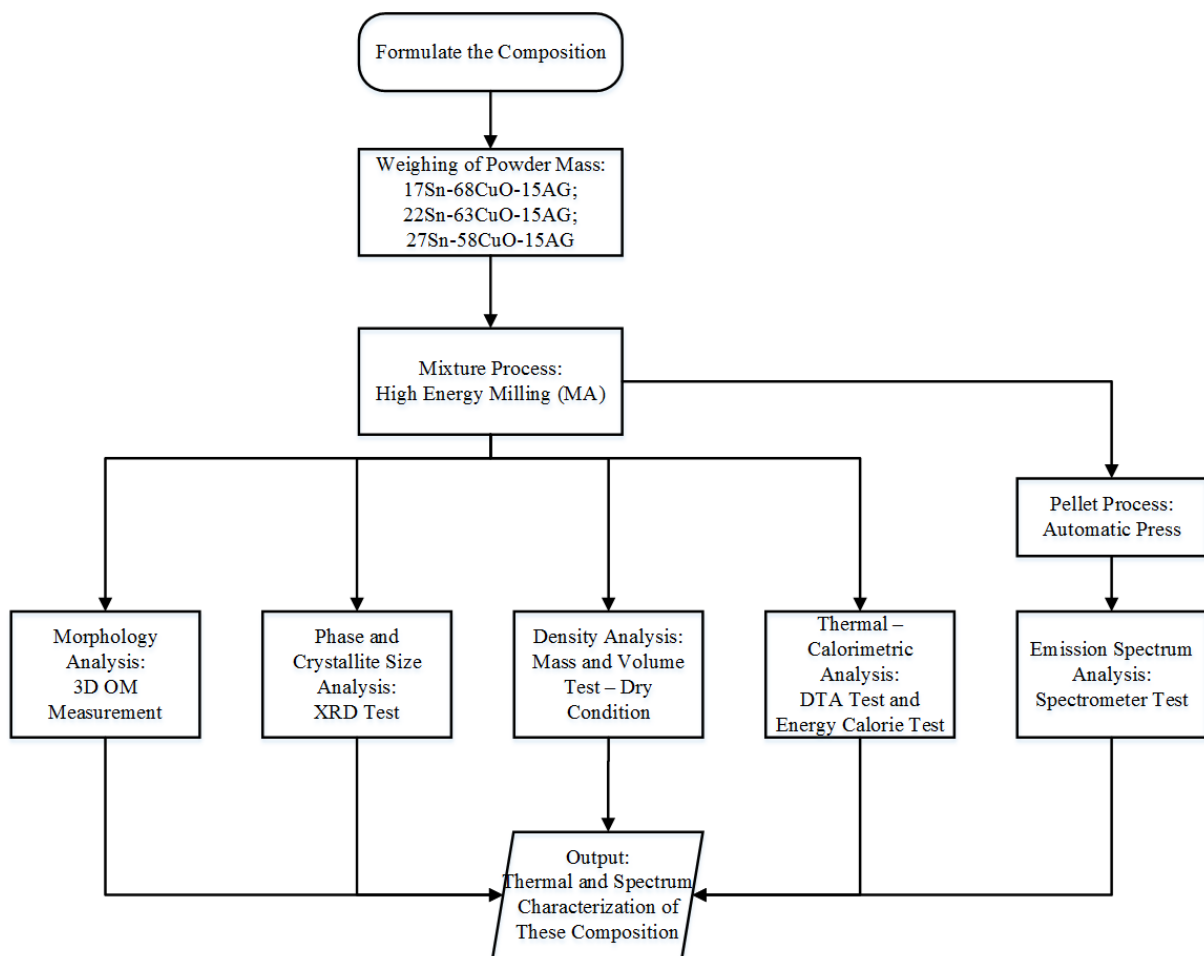

Figure 1. The flowchart of synthesizing and characterization process in this experiment
Source: Processed by Authors, 2020

RESULT AND DISCUSSION
The Morphology and Phase
Figure 2 shows the morphology of xSn-yCuO-zAG (x = 17, 22, and 27%; y = 68, 63, and 58%; and z = 15%). Based on this figure, the 27Sn-58CuO-15AG sample was arranged of white color more than on 22Sn-63CuO-15AG and 17Sn-68CuO-15AG sample, and where this color is a representation for tin and AG existence. It can see in the color of tin and AG powder that used to create these samples. Furthermore, this morphology data is equivalent to the composition of these samples, and where the 27Sn-58CuO-15AG sample has more Sn percentage than 22Sn-63CuO-15AG and 17Sn-68CuO-15AG sample.

Figure 3 shows the peaks of the sample in this research after the XRD measurement. The highest intensity of the peak is 12,500 cps, while the intensity of the baseline in this data is around 1250 cps. So, the intensity ratio between the highest peak and baseline data is 10:1, and where the minimum ratio for good XRD data requirement is 10:1. Therefore, this XRD data is good to use in the next step, phase analysis. Based on the peak, the three sample types are composed of copper oxide (tenoride) phase (PDF-4 = 04-007-0518) and tin phase (PDF-4 = 04-004-7747). This XRD data is also composed of an amorphous Arabic gum amount of 15% at the three samples, and where this amorphous can be seen at an angle of around 20 degrees. From this data, the MA process doesn't generate the new phase, and/or this material in this composition doesn't react to each other.

The increasing Sn composition can generate a higher intensity of the Sn peak. Likewise, the intensity of the CuO peak is more increasing with enhancing of CuO percentage at the sample. Therefore, the Sn peak at the 27Sn-58CuO-15AG sample has an intensity higher than the CuO peak. But at the 17Sn-68CuO-15AG sample, the CuO peak has almost equal intensity with the Sn peak. From morphology and XRD data, the sample in this research is composed of Sn, CuO, and AG phase.

The Density
Table 1 shows the density data of this sample in this research, and where m, r, and t are mass, radius, and height, respectively. Furthermore, samples number 1, 2, and 3 are the representation of 17Sn-68CuO-15AG, 22Sn-63CuO-15AG, and 27Sn-58CuO-15AG, respectively. From this table, the 17Sn-68CuO-15AG sample has the highest density, and the 22Sn-63CuO-15AG sample has a density higher than the 27Sn-58CuO-15AG sample.

Table 1. The density data of 17Sn-68CuO-15AG, 22Sn-63CuO-15AG, and 27Sn-58CuO-15AG sample

No	m (g)	r (cm)	h (cm)	ρ (g/cm^3)
1	1.8233	0.5050	0.5500	4.1361
	1.8232	0.5055	0.5510	4.1202
	1.8232	0.5045	0.5490	4.1516
Mean	1.8232	0.5050	0.550	**4.1359**
2	1.4385	0.5075	0.4790	3.7100
	1.4386	0.5075	0.4789	3.7118
	1.4386	0.5076	0.4790	3.7096
Mean	1.4386	0.5075	0.4790	**3.7105**
3	1.4774	0.5035	0.4970	3.7309
	1.4777	0.5045	0.4980	3.7095
	1.4776	0.5025	0.4980	3.7388
Mean	1.4776	0.5035	0.4977	**3.7264**

Source: Processed by Author, 2020

This density data has a linear correlation with the crystallite size of the highest peak of this sample, and where the crystallite size of 17Sn-68CuO-15AG, 22Sn-63CuO-15AG, and 27Sn-58CuO-15AG sample is 862, 898, and 888 Armstrong, respectively. The highest peak of the three samples is a peak of the tin phase.

The Differential Thermal Analysis
Figure 4 shows the differential thermal analysis (DTA) of 17Sn-68CuO-15AG, 22Sn-63CuO-15AG, and 27Sn-58CuO-15AG samples. From this data, the 17Sn-68CuO-15AG sample generates higher combustion than the 22Sn-63CuO-15AG sample and 27Sn-58CuO-15AG sample, because the exothermic area from this
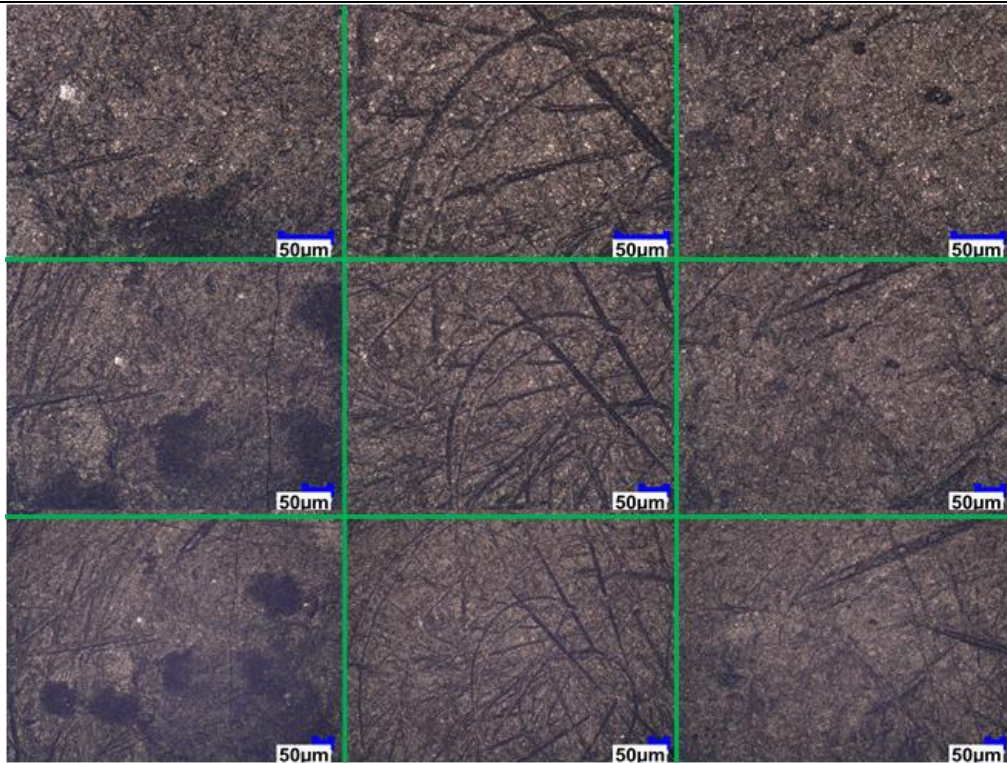
Figure 2. The morphology of 17Sn-68CuO-15AG, 22Sn-63CuO-15AG, and 27Sn-58CuO-15AG sample (left to right) at a magnification of 1000×, 500×, and 300×, respectively (upper to bottom)
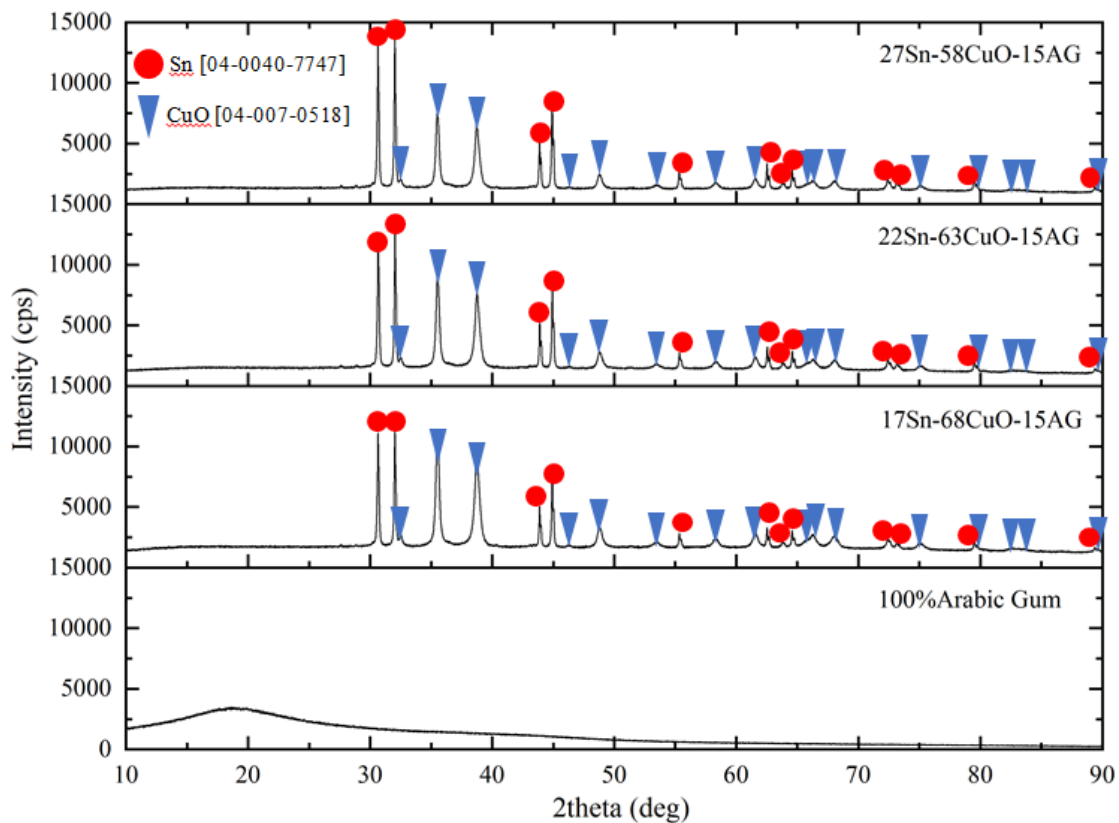*Source:* Processed by Authors, 2020

Figure 3. The XRD data of 17Sn-68CuO-15AG, 22Sn-63CuO-15AG, and 27Sn-58CuO-15AG sample
Source: Processed by Authors, 2020

sample has higher than two other samples, and where the exothermic area has a linear correlation with enthalpy change (ΔH) (Brown, 2004). Furthermore, based on calculation in Origin 2018 software, the exothermic area for 17Sn-68CuO-15AG, 22Sn-63CuO-15AG, and 27Sn-58CuO-15AG sample is 554, 488, and 527 units of area. Therefore, the 17Sn-68CuO-15AG sample has the highest enthalpy change (ΔH).
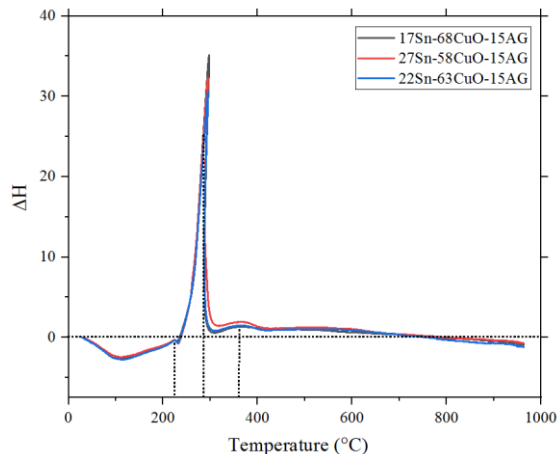

Figure 4. The DTA data of 17Sn-68CuO-15AG, 22Sn-63CuO-15AG, and 27Sn-58CuO-15AG sample
Source: Processed by Authors, 2020

Furthermore, Figure 4 also shows the thermal process at 17Sn-68CuO-15AG, 22Sn-63CuO-15AG, and 27Sn-58CuO-15AG sample is composed of two main endothermic and one main exothermic process. The endothermic process has happened from the temperature of 28 °C until 235 °C, and where the peak temperature of endothermic proses has occurred at a near temperature of 108 °C and 230 °C. This endothermic peak temperature is a representation of melting for Arabic gum (binder) or evaporation of water and tin (fuel), respectively.

This endothermic process generated CO/CO_2 and SnO gas because of the reaction between organic compounds (Arabic Gum)/ fuel (Sn) with oxygen (Hosseini & Eslami, 2011; Tamaekong, Liewhiran, & Phanichphant, 2014), so afterward the exothermic process has occurred. Furthermore, this exothermic

process is a representation of the ignition process in the mixture, and where this process happens at the temperature of 235.1, 236.7, and 237.9 °C for 17Sn-68CuO-15AG, 22Sn-63CuO-15AG, and 27Sn-58CuO-15AG sample, respectively. The 17Sn-68CuO-15AG sample can reach an exothermic process at a lower temperature than the 22Sn-63CuO-15AG sample and 27Sn-58CuO-15AG sample because this sample has the smallest crystallite size. The crystallite size has affected thermal/kinetic rate reaction, and where the smaller crystallite size generates faster thermal/kinetic rate reaction (Adliana, Bura, & Ruyat, 2019; Chaudhary et al., 2015). Hereinafter, based on the average of the four highest peaks of XRD data, the 17Sn-68CuO-15AG, 22Sn-63CuO-15AG, and 27Sn-58CuO-15AG sample have crystallite size of 523.3, 536.5, and 540.8 Armstrong, respectively.

The peak of the ignition process for 17Sn-68CuO-15AG, 22Sn-63CuO15AG, and 27Sn-58CuO-15AG sample occurs at a temperature of 297.4, 295.2, and 295.0 °C, respectively. Therefore, the exothermic process on the 17Sn-68CuO-15AG sample is longer than the 22Sn-63CuO-15AG sample and 27Sn-58CuO-15AG sample. It is due to the 17Sn-68CuO-15AG sample has the highest density, and where based on measurement, the density of 17Sn-68CuO-15AG, 22Sn-63CuO-15AG, and 27Sn-58CuO-15AG sample is 4.13, 3.71, and 3.73 g/cm^3, respectively. Furthermore, the density of material has an effect on the quantity of thermal energy in the material, and where the high-density material usually generated the high-thermal energy (Bofors, 1974). This effect can also see at peak of the three samples, and where the peak of 17Sn-68CuO-15AG, 22Sn-63CuO-15AG, and 27Sn-58CuO-15AG sample reaches ΔT of 35.12, 30.62, and 32.33 seconds, respectively.

Afterward, at the three samples are occurred the decomposition process until the temperature of 315, 317, and 320 °C, respectively. Then the process continues to

exothermic process, and where this process occurs in small form due to the low quantity of fuel in this mixture. After that, this sample reaches the endothermic phase again at a temperature of 775 °C.

Generally, the thermal character of three samples can affect on calorie energy result of each composition. The 17Sn-68CuO-15AG has the greatest calorie energy, and the calorie energy of 27Sn-58CuO-15AG is higher than 22Sn-63CuO-15AG. The energy calorie of each this material is 500.31, 373.73, and 450.33 Cal. The quantity of calorie energy can impact the damage of a projectile jacket. The lower-calorie energy can avoid a crack in the projectile jacket, and it can minimize accidents on the user. Therefore, from the calorie, energy aspect, the composition of 22Sn-63CuO-15AG is the most reliable for avoiding crack on the projectile.

The Spectrum
Based on Figure 5, the spectrum data of the 17Sn-68CuO-15AG, 22Sn-63CuO-15AG, and 27Sn-68CuO-15AG sample shows these samples emitted wavelength of 610 – 930 nm. This wavelength is a representation of red color and infrared spectrum. The spectrum of 620 – 750 nm is a range of red color, while the spectrum of 750 – 930 nm is including in the infrared range.

Furthermore, the composition of this sample can enhance the intensity of the flame, it is can be seen at some primary peaks of the flame such as in wavelength of around 588 nm, 765 nm, and 943 nm, the intensity of the flame can increase because of this material existence, and this case probably because increasing of quantity (percentage) of CuO (see Figure 5).

From this spectrum measurement, the combination of the Sn-CuO-AG sample emits a strong signal in the infrared range (start from 800 nm), but in the red color spectrum, this sample does not emit strong red color, especially at the 27Sn-58CuO-15AG sample. It is can be seen at the
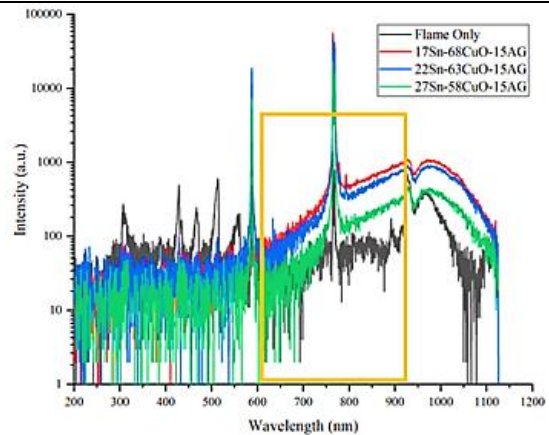

Figure 5. The spectrum data of Flame, 17Sn-68CuO-15AG, 22Sn-63CuO-15AG, and 27Sn-58CuO-15AG sample
Source: Processed by Author, 2020

wavelength of 610 - 700 nm, and where the signal at this range is wider than the wavelength of > 700 nm.

From Figure 6–8, an increase of Sn percentage has a big contribution to produce this wider signal, especially at the wavelength range of 600 – 700 nm. Probably, it due to the color emission of the tin, and where tin has yellow color emission, the wavelength of 570 – 590 nm (Henry & Laird, 2014). So, increasing Sn content probably can bother color emission of CuO, because interference and/or resonance destruction happen. Besides that, the reaction between Sn and oxygen in the exothermic process can generate SnO material, and where the increase of Sn percentage probably can increase the formation of SnO. Furthermore, the increasing of SnO quantity can improve the absorption in the visible spectrum region and affects the peak of emission intensity (Masai, Takahashi, & Fujiwara, 2009; Yin et al., 2019).

Moreover, the decreasing of Sn (fuel) addition on this composition is enhancing the intensity at the infrared spectrum. It is can be seen at a wavelength of 793 nm, and where the intensity of the signal at this wavelength increased in mini-peak form (see Figure 9). Furthermore, this peak can be seen at Sn composition below 23%.

Based on the calorie energy, enthalpy change, and emission spectrum data, the
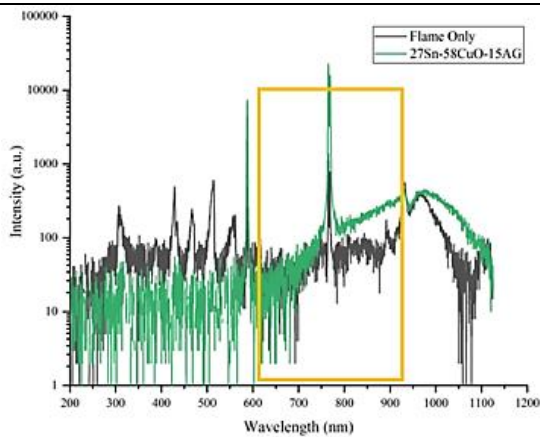
Figure 6 The spectrum data of Flame and 27Sn-58CuO-15AG sample
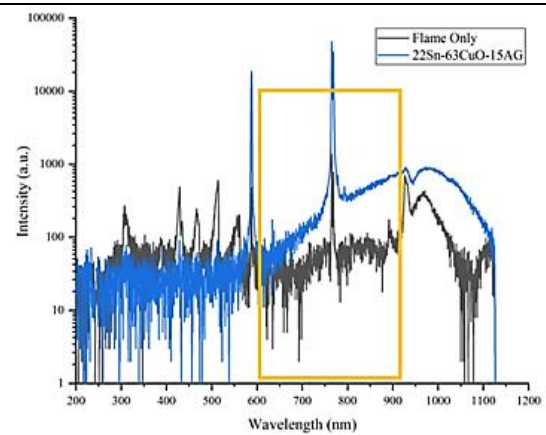*Source:* Processed by Authors, 2020

Figure 7 The spectrum data of Flame and 22Sn-63CuO-15AG sample
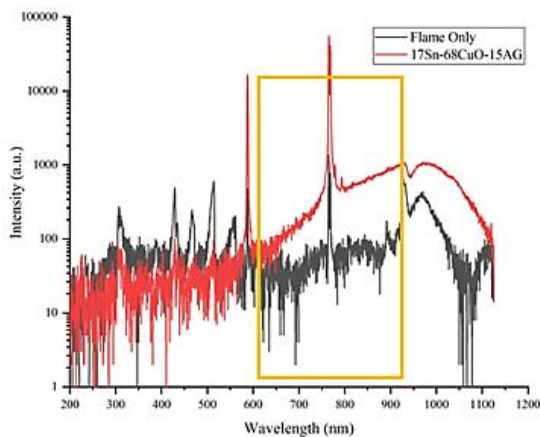*Source:* Processed by Authors, 2020

Figure 8 The spectrum data of Flame and 17Sn-68CuO-15AG sample
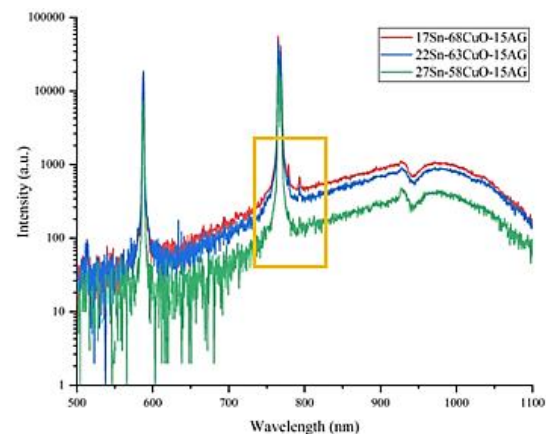*Source:* Processed by Authors, 2020

Figure 9 The spectrum data of 17Sn-68CuO-15AG, 22Sn-63CuO-15AG, and 27Sn-58CuO-15AG sample
Source: Processed by Authors, 2020

composition of the 22Sn-63CuO-15AG sample has the lowest exothermic energy, medium ignites temperature and the strongest red spectrum emission. The tracer projectile with the lowest calorie energy can prevent the jacket of the projectile from damage due to excess heat energy. If the jacket projectile broke, so the projectile fails to shoot on the target, and this projectile can go to the user or other person around the user. Furthermore, the strong red emission of the tracer projectile can assist the user in observing the rate of this tracer projectile, and gives the sign to the friend regarding the location of the enemy.

CONCLUSIONS, RECOMMENDATION, AND LIMITATION

From this research, the 22Sn-63CuO-15AG composition has red color as strong as the 27Sn-58CuO-15AG composition, but stronger than the 17Sn-68CuO-15AG composition. Furthermore, the 22Sn-63CuO-15AG composition has the lowest exothermic energy and the least calorie energy. This composition has medium ignition compared to the composition of 17Sn-68CuO-15AG and 27Sn-58CuO-15AG, and where the sample of 17Sn-68CuO-15AG has the fastest ignition.

Furthermore, the parameter is affecting

on the spectrum and exothermic energy of the Sn-CuO-AG composition:

a. Sn quantity; the Sn material with a percentage of more than 27% generates the wider signal (weak signal) at this tracer composition.

b. Crystallite size; the smaller crystallite size generates the earlier ignite temperature, in this case, the 17Sn-68CuO-15AG sample has the smallest crystallite size (862 Armstrong) can result in the earliest ignite temperature.

c. Density; the higher density can produce a higher exothermic energy area, in this case, the 17Sn-68CuO-15AG sample has the biggest density (4.14 g/cm^3) can produce the biggest area of exothermic energy and the greatest calorie energy.

The composition of 22Sn-63CuO-15AG is the reliable composition for tracer projectile in medium caliber, compared to two other compositions. But, this composition must be added to more oxidizer material such as potassium perchlorate, so this composition can generate a low flash point or can ignite in small heat. If the more oxidizer material, so the tracer projectile can easily ignite. It is important to make the tracer composition can compatible with a small-caliber. Since the ignite composition in the small caliber has emitted low burning temperature, around 300 °C.

REFERENCES

Adliana, N., Bura, R. O., & Ruyat, Y. (2019). Analisis pengaruh karakteristik propelan terhadap balistik interior pada munisi kaliber kecil. *Teknologi Persenjataan*, *1*(1), 39–62.

Agrawal, J. P. (2010). *High Energy Materials: Propellants, Explosives, and Pyrotechnics* (First). New Delhi: Wiley-VCH.

Anderson, C. S. (2020). Tin. *U.S. Geological Survey*, (1), 1–2.

Bailey, A., & Murray, S. G. (2000). Explosives, Propellants, and Pyrotechnics. Brassey's London. Retrieved from http://books.google.com/books?id=hANUAAAAMAAJ&pgis=1

Bofors, A. (1974). *Analytical Methods for Powders and Explosives*. Bofors AB Bofors.

Brown, M. E. (2004). *Introduction to Thermal Analysis: Techniques and Application*. Kluwer Academics Publisher. Retrieved from http://ebooks.springerlink.com

Buc, S. M., Adelman, G., & Adelman, S. (1993). *Development of Alternate 7.62 mm Tracer Formulations* (Vol. OMB No. 07). Maryland. https://doi.org/10.1090/dimacs/029/20

Chaudhary, A. L., Sheppard, D. A., Paskevicius, M., Pistidda, C., Dornheim, M., & Buckley, C. E. (2015). Reaction kinetic behaviour with relation to crystallite/grain size dependency in the Mg-Si-H system. *Acta Materialia*, *95*, 244–253. https://doi.org/10.1016/j.actamat.2015.05.046

Conkling, J. A., & Mocella, C. J. (2019). *Chemistry of Pyrotechnics: Basic Principles and Theory* (Third). CRC Press: Taylor & Francis Group. https://doi.org/10.1201/9780429262135-10

Crouch, I. G. (2019). Body armour – New materials, new systems. *Defence Technology*, *15*(3), 241–253. https://doi.org/10.1016/j.dt.2019.02.002

Douda, B. E. (1964). *Theory of colored flame production* (Vol. RDTN No. 7).

Ellern, H. (1968). *Military and Civilian Pyrotechnics* (First). Chemical Publishing Company, Inc.

Garner, J., Huang, X., Mishock, J., & Kostka, J. (2009). *A Tracer Analysis for the M1002 Training Projectile*.

Henry, D. J., & Laird, D. W. (2014). *How old is my bronze cannon? A laboratory exercise linking*

analytical chemistry, spectroscopy, and metallurgy. Journal of Laboratory Chemical Education (Vol. 2). https://doi.org/10.5923/j.jlce.201402 04.04

Hosseini, S. G., & Eslami, A. (2011). Investigation on the reaction of powdered tin as a metallic fuel with some pyrotechnic oxidizers. *Propellants, Explosives, Pyrotechnics*, *36*(2), 175–181. https://doi.org/10.1002/prep.2009000 82

ITRI. (2020). Global resources and reserves: security of long term tin supply. *Industrial Technology Research Institute*, 1–23.

Masai, H., Takahashi, Y., & Fujiwara, T. (2009). Addition effect of SnO in optical property of Bi2 O3 - containing aluminoborate glass. *Journal of Applied Physics*, *105*(083538). https://doi.org/10.1063/1.3115472

Meyerriecks, W., & Kosanke, K. L. (2003). Color Values and Spectra of the Principal Emitters in Colored Flames. *Journal of Pyrotechnics*, (18), 710–731.

National Research Council. (2003). *Materials Research to Meet 21st Century Defense Needs*. *Materials Research to Meet 21st Century Defense Needs*. Washington D.C: National Academies Press. https://doi.org/10.17226/10631

Sadek, R., Kassem, M., Abdo, M., & Elbasuney, S. (2016). Spectrally Adapted Red Flares With Enhanced Color Quality and Luminous Intensity. *The International Conference on Chemical and Environmental Engineering*, *8*(13), 282–303. https://doi.org/10.21608/iccee.2016.3 5126

Sadek, R., Kassem, M., Abdo, M., & Elbasuney, S. (2017). Novel yellow colored flame compositions with superior spectral performance. *Defence Technology*, *13*(1), 33–39. https://doi.org/10.1016/j.dt.2016.12.0 01

Tamaekong, N., Liewhiran, C., & Phanichphant, S. (2014). Synthesis of thermally spherical CuO nanoparticles. *Journal of Nanomaterials*, 1–5. https://doi.org/10.1155/2014/507978

Yin, G., Sun, J., Zhang, F., Yu, W., Peng, F., Sun, Y., … He, D. (2019). Enhanced gas selectivity induced by surface active oxygen in SnO/SnO 2 heterojunction structures at different temperatures. *RSC Advances*, *9*(4), 1903–1908. https://doi.org/10.1039/c8ra09965k